



HAL
open science

A Semi-Elliptical UWB Folded Dipole Antenna

Romain Greard, Mohamed Himdi, Dominique Lemur, Gwenal Le Dem, Pierre Thaly, Cyrille Le Meins

► **To cite this version:**

Romain Greard, Mohamed Himdi, Dominique Lemur, Gwenal Le Dem, Pierre Thaly, et al.. A Semi-Elliptical UWB Folded Dipole Antenna. *Electronics*, 2023, 12 (13), pp.2788. 10.3390/electronics12132788 . hal-04192461

HAL Id: hal-04192461

<https://hal.science/hal-04192461>

Submitted on 31 Aug 2023



HAL is a multi-disciplinary open access archive for the deposit and dissemination of scientific research documents, whether they are published or not. The documents may come from teaching and research institutions in France or abroad, or from public or private research centers.

L'archive ouverte pluridisciplinaire **HAL**, est destinée au dépôt et à la diffusion de documents scientifiques de niveau recherche, publiés ou non, émanant des établissements d'enseignement et de recherche français ou étrangers, des laboratoires publics ou privés.



Distributed under a Creative Commons Attribution 4.0 International License

A Semi-Elliptical UWB Folded Dipole Antenna

Romain Greard ^{1,*} , Mohamed Himdi ¹ , Dominique Lemur ¹, Gwenal Le Dem ², Pierre Thaly ²
and Cyrille Le Meins ²

- ¹ Institut d'Electronique et des Technologies du numeRique (IETR), Université de Rennes, 35000 Rennes, France; mohamed.himdi@univ-rennes.fr (M.H.); dominique.lemur@univ-rennes.fr (D.L.)
² THALES SIX GTS France, 49309 Cholet, France; gwenal.colosioledem@thalesgroup.com (G.L.D.); pierre.thaly@thalesgroup.com (P.T.); cyrille.lemeins@thalesgroup.com (C.L.M.)
* Correspondence: romain.greard@univ-rennes.fr

Abstract: In this paper, a novel structure of a semi-elliptical folded dipole for ultra-wideband (UWB) receiving applications is discussed. This proposed antenna has a directive radiation pattern resulting in a high gain over the bandwidth. The design uses a planar technology including a microstrip line to slot line transition and optimized curves to obtain a measured impedance bandwidth of 2.3–26 GHz with the condition of $S_{11} < -6$ dB (level accepted for receiving antenna) and meets $S_{11} < -10$ dB in several bands. Additionally, the simulated gain ranges from 5 dBi to 9.5 dBi across the entire bandwidth with an efficiency of at least 75%. This antenna model offers a reconfiguration capability. The symmetrical feeding used in this antenna creates the directive behavior. Characteristics of this semi-elliptical folded dipole antenna make it suitable for modern wireless communications, such as 5 G around 3.5 GHz, and easy to integrate in antenna arrays (MIMO systems). The four ports of the antenna also make it a candidate for radiation pattern reconfigurability applications reducing in this way the number of elements in network antennas.

Keywords: UWB; folded dipole; directive antenna



Citation: Greard, R.; Himdi, M.; Lemur, D.; Le Dem, G.; Thaly, P.; Le Meins, C. A Semi-Elliptical UWB Folded Dipole Antenna. *Electronics* **2023**, *12*, 2788. <https://doi.org/10.3390/electronics12132788>

Academic Editor: Reza K. Amineh

Received: 28 April 2023

Revised: 19 June 2023

Accepted: 22 June 2023

Published: 24 June 2023



Copyright: © 2023 by the authors. Licensee MDPI, Basel, Switzerland. This article is an open access article distributed under the terms and conditions of the Creative Commons Attribution (CC BY) license (<https://creativecommons.org/licenses/by/4.0/>).

1. Introduction

Following the Federal Communications Commission's (FCC) allocation of the frequency band 3.1 GHz to 10.6 GHz for commercial communication applications in 2002 [1], ultra-wideband (UWB) systems have emerged as a significant area of interest in the electronics industry. There are plenty of applications in diverse domains, such as telecommunications, medical, space and military fields [2,3]. Various types of antennas, such as horns, log-periodic antennas, conical antennas, planar monopoles and dipoles, have been extensively studied to achieve wide bandwidths [4–8]. These antennas offer optimized transitions from feeding to free space.

Printed antennas are widely chosen in ultra-wideband applications due to their numerous advantages, including small size, low cost, high radiation efficiency and simple design and production. To meet the specific requirements of different applications, it is common to employ different modifications of geometry. Typically, square, cylindrical, elliptical, or even fractal shapes are good examples to extend the impedance bandwidth of monopole and dipoles antennas [9–13]. Another technique for modifying antenna impedance involves folding the structure over a ground plane, allowing for optimization of the bent structure to yield improved outcomes. This folding technique can also control the orientation of surface currents [14] and enable control over radiation direction. Recent studies on planar folded dipoles have achieved bandwidths ranging from one to several octaves [15–17]. In those examples, only microstrip feed lines have been used. This solution is the simplest way to feed an antenna with an asymmetrical wave. However, these examples of folded antennas do not offer any reconfiguration possibilities.

In this study, an elliptical folded dipole antenna design for Ultra-Wide Band (UWB) applications is discussed. The optimized folded monopole shape is used as the basis for the antenna design, and previous studies [18–21] have examined the folding of thick monopoles and dipoles over a ground plane to enlarge the impedance bandwidth. Parameters such as the thickness of the fed and the folded wires were according to [18–21]. Stabilization of the radiation pattern of the antenna is achieved by adding a second strand with vertical symmetry. This idea is in opposition to the common folded dipole which includes a horizontal symmetry. It converts the monopole structure into a dipole one. The proposed antenna has four ports which offers reconfigurability. We chose to connect two of them to the ground. Depending on the choice of the feed, symmetrical or asymmetrical, the radiation behavior is modified. Feeding the antenna with a symmetric ($0^\circ/180^\circ$) wave using a microstrip line to slot line transition [22–24] results in a directive radiation pattern. In this paper, different configurations are presented but only the directive version has been fully realized and measured. Applications related to wireless communications such as 5 G (3.5 GHz bands) or antenna arrays requiring directive radiating elements are considered (indoor/outdoor communications). The proposed antenna exhibits an impedance bandwidth of 2.3 GHz to 26 GHz+ when $S_{11} < -6$ dB, with a maximum gain of 9.5 dBi at 6.6 GHz. For more common communications applications, this antenna achieves the $S_{11} < -10$ dB condition in the bands 3.3–8 GHz, 9.8–12.6 GHz and 13.1–26 GHz. However, at high frequencies (>12 GHz), the directional behavior of this folded dipole antenna is not fully verified. A significant cross-polarization and lateral radiation are observed.

2. Folded Structures and Feeding

2.1. Large Folded Monopole

A large folded monopole of $\lambda/4$ in length is comparable with a conventional monopole in many points. In particular, the radiation pattern has a toroidal shape at the resonance frequency f_r (Figure 1a). The monopole can be bent to affect this radiation. In Figure 1b, bending the antenna over a ground plane results in a main beam with a significant steering at $f = 2 f_r$, while the pattern is still toroidal at lower frequencies. At $f = 5 f_r$, the null on the axis of the structure is now replaced by a maximum of radiation. This is a technique to obtain a directive antenna in a precise direction at a specific frequency.

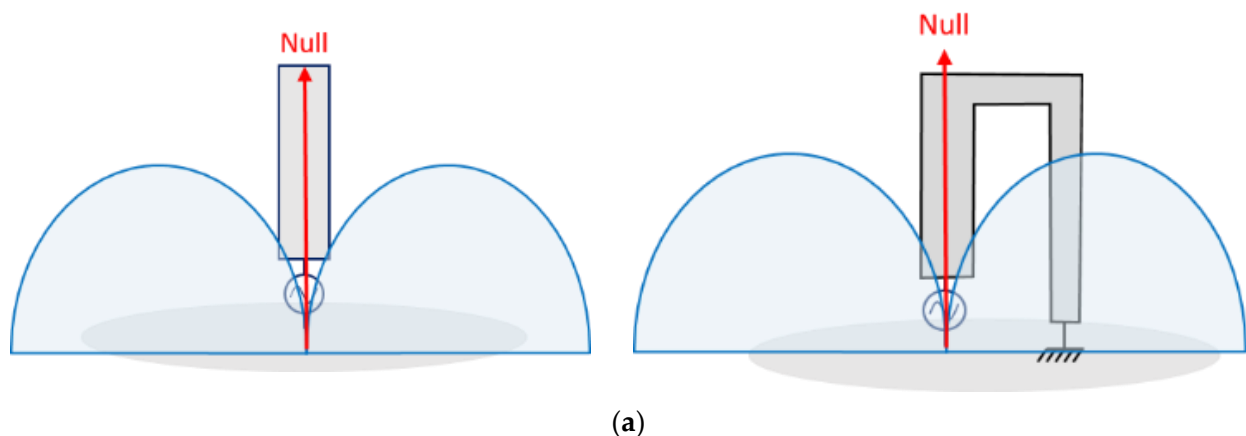


Figure 1. Cont.

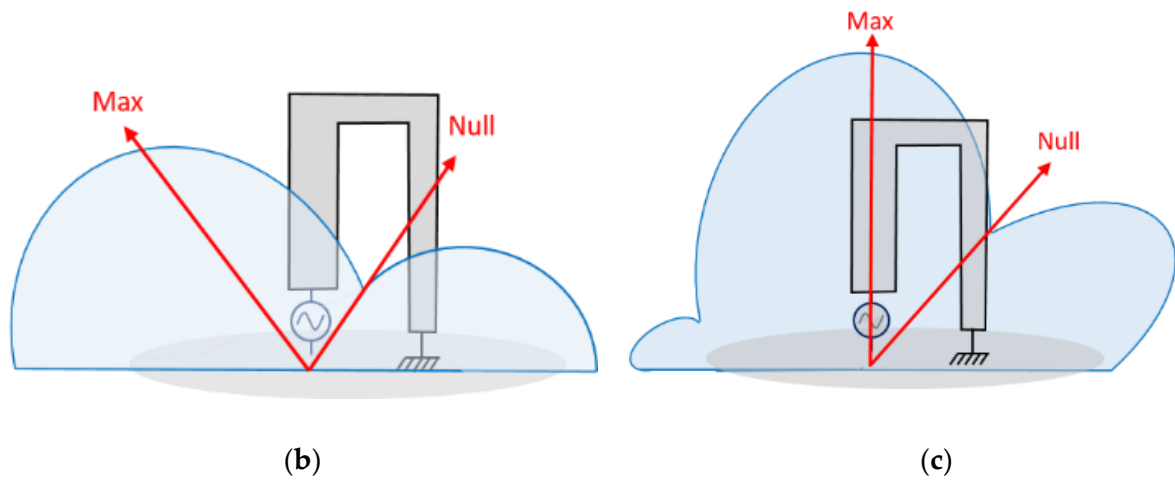


Figure 1. Thick monopole and folded monopole and their radiation pattern (a) at $f = fr$ and folded monopole at $f = 2 fr$ (b) and $f = 5 fr$ (c).

2.2. Large Folded Dipole and Symmetrical Feeding

The classic toroidal radiation pattern of the monopole and dipole can be restored throughout the frequency range $fr < f < 5 fr$ by making the structure symmetrical. The conventional folded dipole is designed along a horizontal plane of symmetry, as shown in Figure 2a, but in this paper, we propose to implement this symmetry along a vertical axis and keep the horizontal ground plane (Figure 2b).

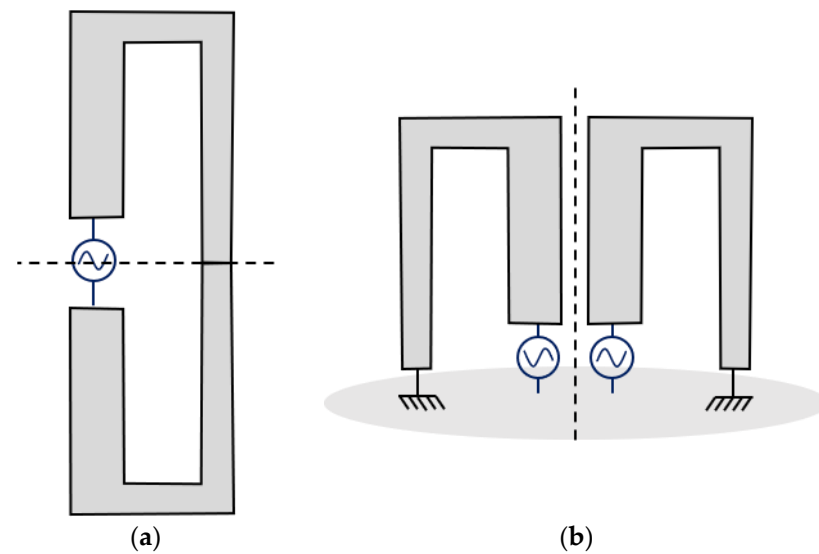


Figure 2. Representation of the classical folded dipole (a) and the folded dipole with vertical symmetry (b).

Consequently, when both arms of the antenna are excited with an asymmetrical wave (unbalanced wave), no radiation is observed along the axis of symmetry of the dipole (Figure 3a). We retrieve the typical dipole pattern. However, to obtain a directive behavior, a 180° phase shift is applied to the two arms. As a result, a maximum radiation is now observed along the axis of symmetry in the same frequency range $fr < f < 5 fr$. By analyzing the electrical currents, we observe that in the case of an asymmetrical feeding, the currents I_2 on the two arms of the antenna are opposite. This causes a null of radiation in the axis of the antenna (Figure 3a). However, with a symmetrical feeding (Figure 3b), these two currents add up, which explains the maximum of energy in the axis of the dipole. This

maximum is located in the vertical axis because the value of the phase shift is 180° . It is possible that other values such as 90° (or -90°) could redirect this maximum on the right horizontal axis (or left horizontal axis). In other words, using a $90^\circ / -90^\circ$ coupling circuit, diodes circuits, or even a switch, this antenna design can be seen as a reconfigurable antenna and can still have a directive radiation pattern as mentioned in Figure 4a and b. Otherwise, this behavior is only valid on a narrow band which depends mainly on the antenna height.

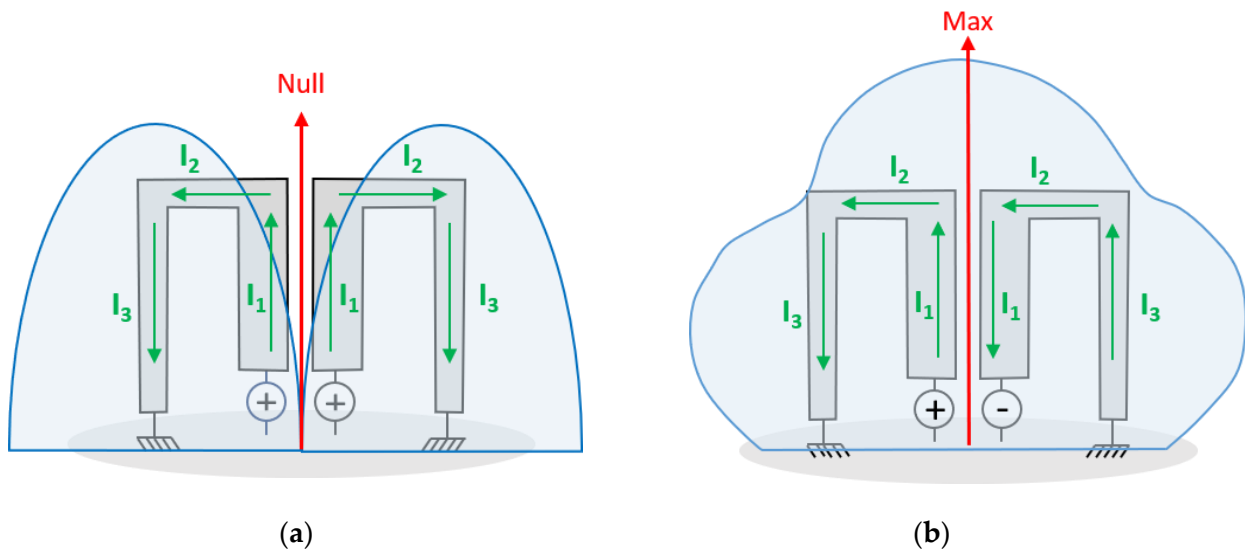


Figure 3. Folded dipole with (a) asymmetrical and (b) symmetrical feeding and their respective radiation pattern.

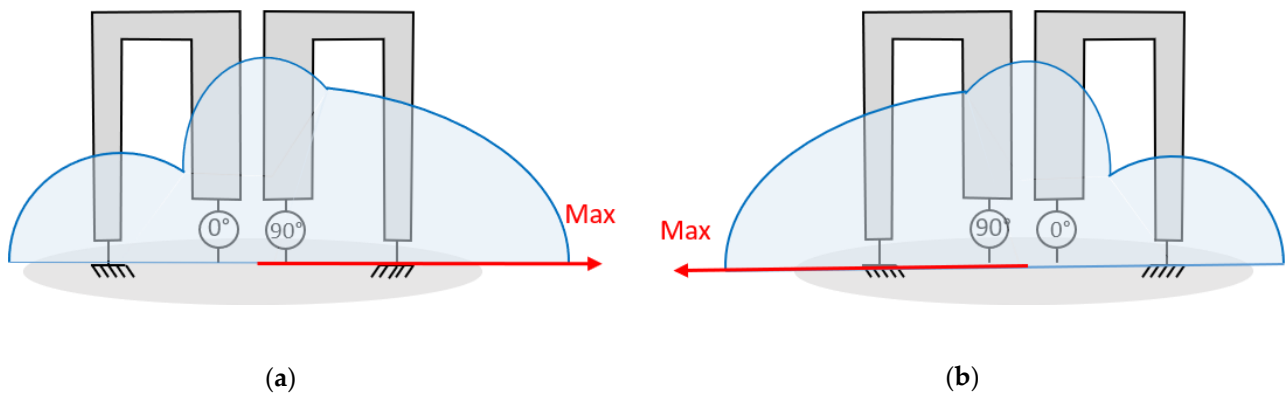


Figure 4. Folded dipole with (a) $0-90^\circ$ feeding and (b) $90-0^\circ$ feeding and their respective radiation pattern.

This paper only reports on the directive version with a 180° phase difference power supply, since it offers a stable directional behavior over a larger frequency range than the monopole versions. However, work on the reconfigurability aspect of this folded antenna (switch, pin diode, coupling circuit) is in progress, also the beam direction can change with the feed phase difference which could be the subject of a future communication.

3. Design and Simulation

3.1. Semi-Elliptical Monopole to Dipole Design

Earlier in the text, we discussed monopoles and dipoles in three dimensions (thick monopoles and dipoles). However, in this paper, we focus only on optimizing planar

structures due to their simplified production process and their satisfying performance in terms of matching and radiation. The shape of a semi-elliptical folded monopole antenna that conforms to the principles outlined in the preceding paragraphs, matched to 150Ω , is shown in Figure 5a. This bending is made of one semi-ellipse and a semi-ellipse hollow. These shapes were chosen because they are known to offer wide bandwidths. The ellipse that defines the outer line has a 0.6 elliptical ratio. The planar structure stands over a ground plane and ends in a short circuit. Various elliptical curves and thicknesses of the monopole were investigated, and the optimal values are outlined in Table 1. The height b_2 and the width of the outer ellipse are the dimensions that will mainly define the low frequency of the impedance bandwidth. The inner elliptical trough (hollow), defined by the dimensions a_1 and b_1 , stabilizes the low frequency behavior by changing the current distribution. The currents located on the right edge of the design (Figure 5a) increase with the size of the hollow. To form a dipole, we simply add the symmetrical shape about a vertical plane, as illustrated in Figure 5b. Two of the four ports are grounded, while the two others are connected to the feeding circuit. The gap (g) between the two strands is optimized and produces a 50Ω matched access. The type of feeding, whether asymmetrical or symmetrical, determines whether it is a null or maximum radiation.

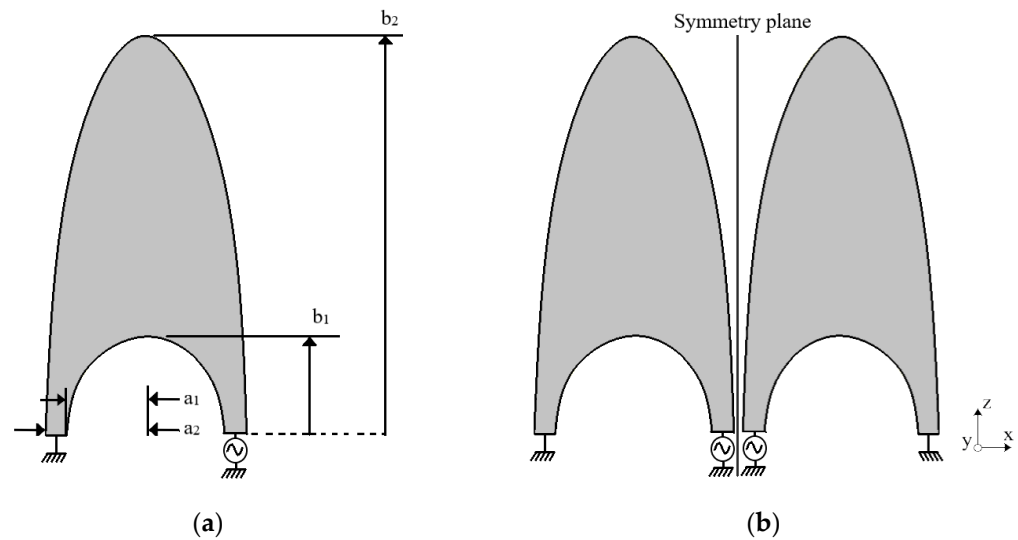


Figure 5. Planar monopole (a) and dipole (b) structures. a_1 and b_1 represent the inner ellipse dimensions, a_2 and b_2 the outer ellipse.

Table 1. Optimized dimensions of the proposed antenna.

Parameters	Value (mm)
a_1	16
a_2	20
b_1	20
b_2	80
g	0.3
r_1	2
l_1	18.4
l_2	8.85
l_3	53
w_1	4.1
w_2	4.2
r	5.42
θ	180°

The final design of the folded dipole, obtained by the approach explained in Section 2, is similar to a Vivaldi antenna. The common tapered shape of these two antennas allows a very wide band matching.

In other words, as explained in Section 2, the phase shift means that the antenna's maximum radiation is off-point. The radiation of several simulated configurations is shown in Figure 6 in the Oxz plane. The case of an in-phase feeding on both wires ($0-0^\circ$), implies radiation identical to that of a dipole. This behavior is broadband. If we choose a phase shift between 0° and 180° , then we obtain beam steering. In the presented results, at the lowest frequency where the antenna is well matched (1.6 GHz), the steering is around 90° . As the phase shift increases, radiation at 0° appears until it is in the majority when the feed is symmetrical ($0-180^\circ$). As mentioned earlier, only the directional behavior of the model fed by a $0-180^\circ$ (or $0-0^\circ$) wave is valid over a wide band.

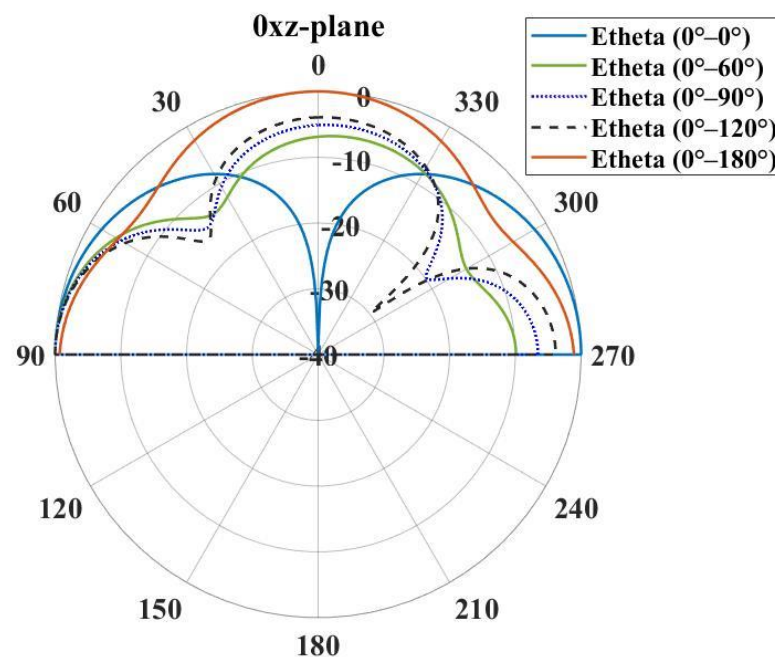


Figure 6. Simulations of radiation pattern at lower frequencies with different feed phase difference (at 1.6 GHz).

3.2. Microstrip Line to Slot Line Transition

To obtain a maximum radiation in the z-axis, a solution is to feed the two strands of the dipole with a symmetrical wave. In other words, a 180° phase shift feeding circuit must be attached at the bottom of the structure. A proposed method is to feed the antenna using a 50Ω microstrip line that terminates on an open circuit stub. This line excites the slot between the two arms of the dipole, as depicted in Figure 7b. The difference of potential at these two points of the line results in the creation of a voltage between the two strands, which means that the current is in opposition. However, the transition is a crucial factor in limiting the impedance bandwidth of this type of structure and therefore requires optimization.

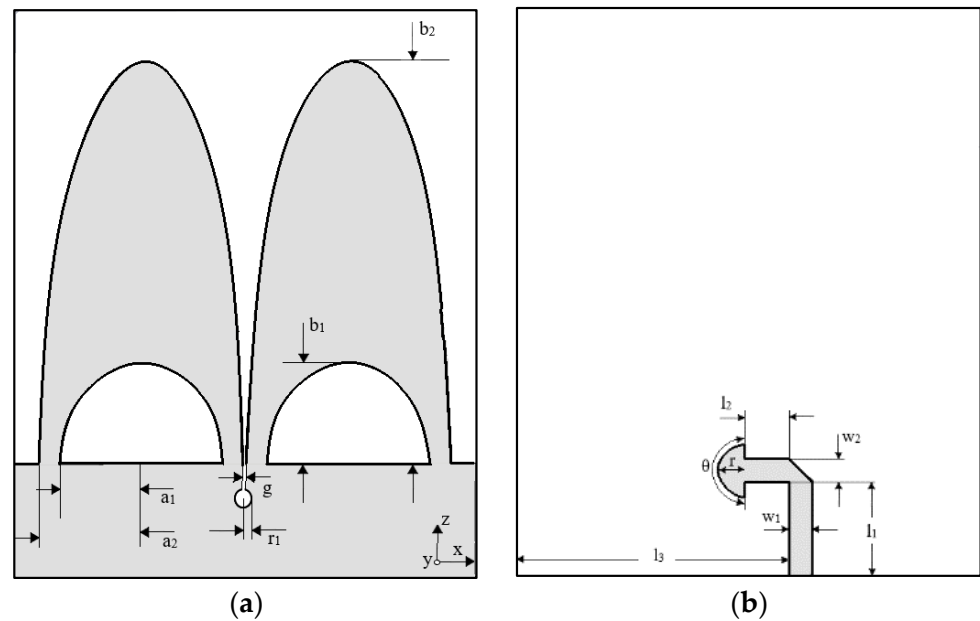


Figure 7. Geometry of the folded dipole fed by microstrip line to slot line transition: (a) top view, (b) bottom view.

A parametric study on various design parameters of the transition is performed to maximize the frequency range of the antenna. In Figure 8, different l_1 lengths are under study. This length impacts the stub position on the slot which changes the impedance matching. Several options are available, depending on the frequency range required. Figure 9 shows the reflection coefficient of a few stub angles (θ). The wider the angle is, the more the S_{11} is improved, except for the 8–10 GHz frequency range. By combining those results with other minor parametric simulations, we determine the optimized parameters. For example, in this semi-elliptical folded dipole, the combination $l_1 = 18.4$ mm and $\theta = 180^\circ$ gave us the best results so far on the whole 2.3–26 GHz frequency range. A_1 and b_1 are the dimensions (height and width) of the inner semi-ellipse when a_2 and b_2 are the ones of the outer semi-ellipse.

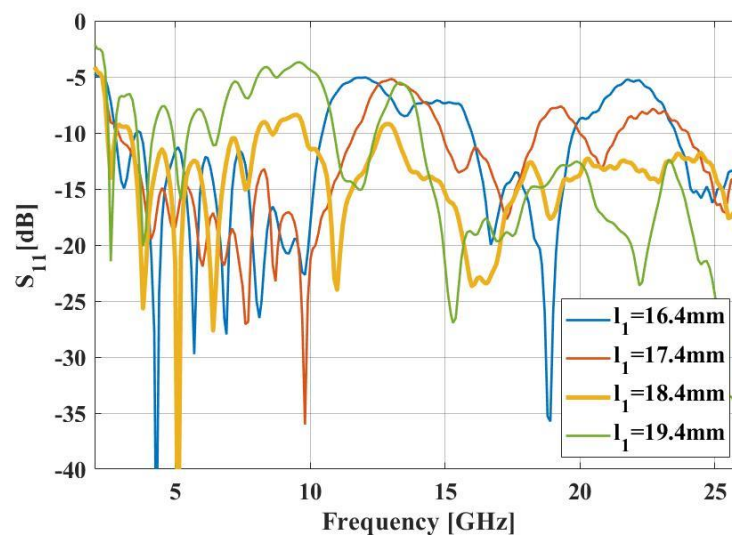


Figure 8. Variation of reflection coefficient for different l_1 lengths.

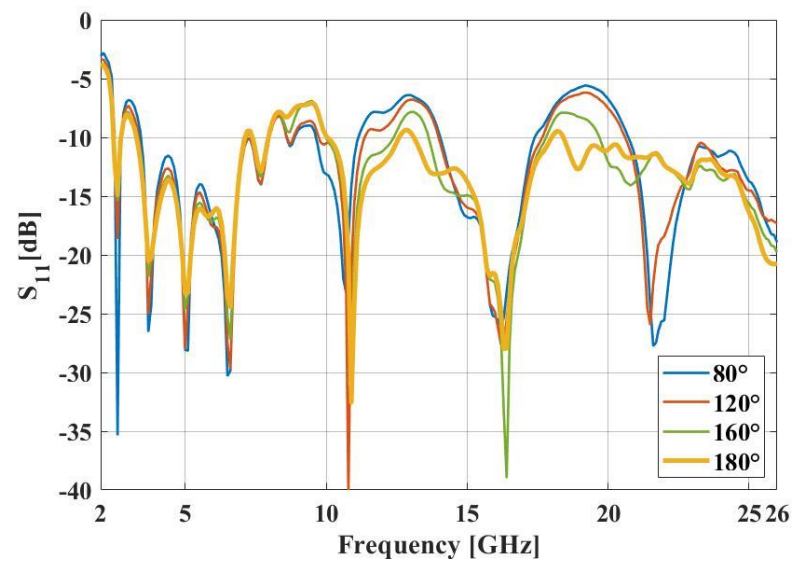


Figure 9. Variation of reflection coefficient for different stub angles (θ).

4. Simulation and Measurement

The performance of the semi-elliptical folded dipole antenna, shown in Figure 7, is optimized and simulated using CST Studio Suite. All the parameter values are detailed in Table 1. The substrate used on this antenna design is Rodger R4003C ($\epsilon_r = 3.38$, $h = 1.52$ mm). Figure 10 depicts the prototype of the semi-elliptical folded dipole. The reflection coefficient of the structure is illustrated in Figure 11a. The semi-elliptical dipole has an impedance bandwidth of 2.3 GHz to 25 GHz under the condition of $S_{11} < -6$ dB, making it suitable for reception purposes. However, for more restrictive applications, the presented model meets the $S_{11} < -10$ dB condition over several bands, including 3.3–8 GHz, 9.8–12.6 GHz and 13.1–26 GHz.

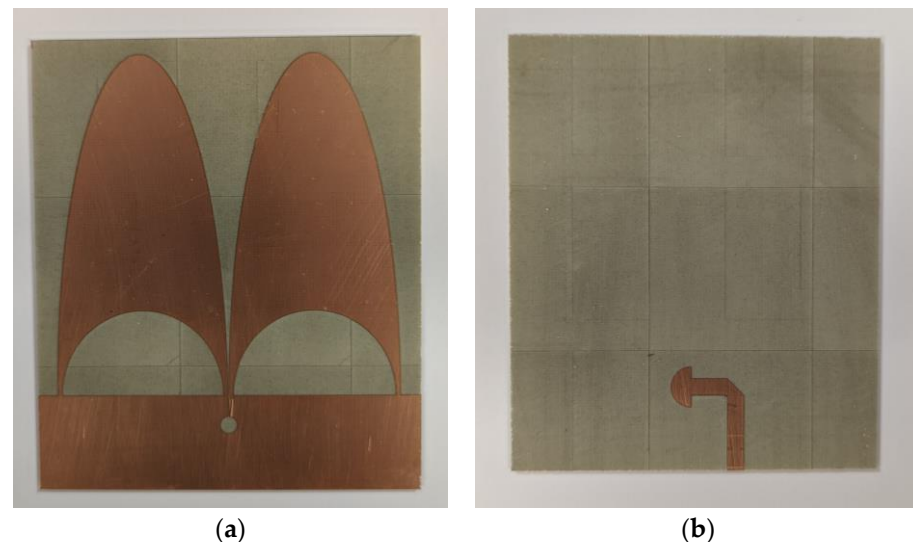


Figure 10. Prototype of the folded dipole antenna: (a) top view, (b) bottom view.

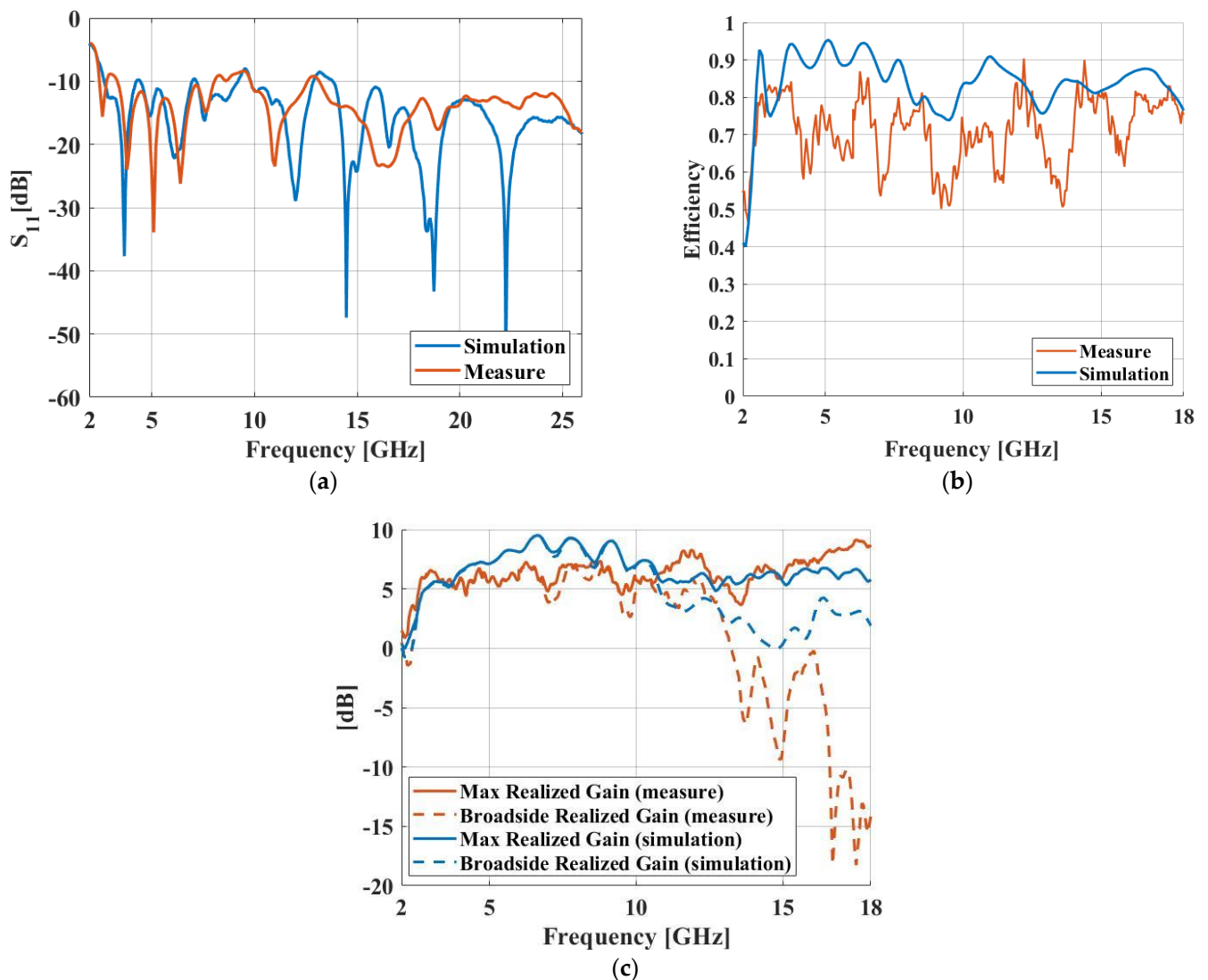


Figure 11. Measured and simulated performances of the semi-elliptical dipole: (a) reflection coefficient, (b) radiation efficiency and (c) max gains.

The simulation results for the radiation and total efficiencies of the dipole antenna are presented in Figure 11b. The total efficiency is greater than 75% across the entire bandwidth starting at 2.3 GHz. The proposed structure has directional radiation, resulting in a high maximum gain of 9.5 dBi at 6.6 GHz (Figure 11c), located in the z-axis (broadside). However, above 12 GHz, the maximum radiation is no longer in this direction, and the steering of the main beam and high cross-polarization are observed but not shown in this paper. In this way, broadband radiation behavior is achieved up to 12 GHz. However, for applications that do not require directional radiation (IOT, UWB impulse systems), where the gain remains high, the semi-elliptical folded dipole antenna may be perfectly suitable above 12 GHz. Simulated radiation patterns showing the directional behavior in the 2–10 GHz band are mentioned in Figure 12.

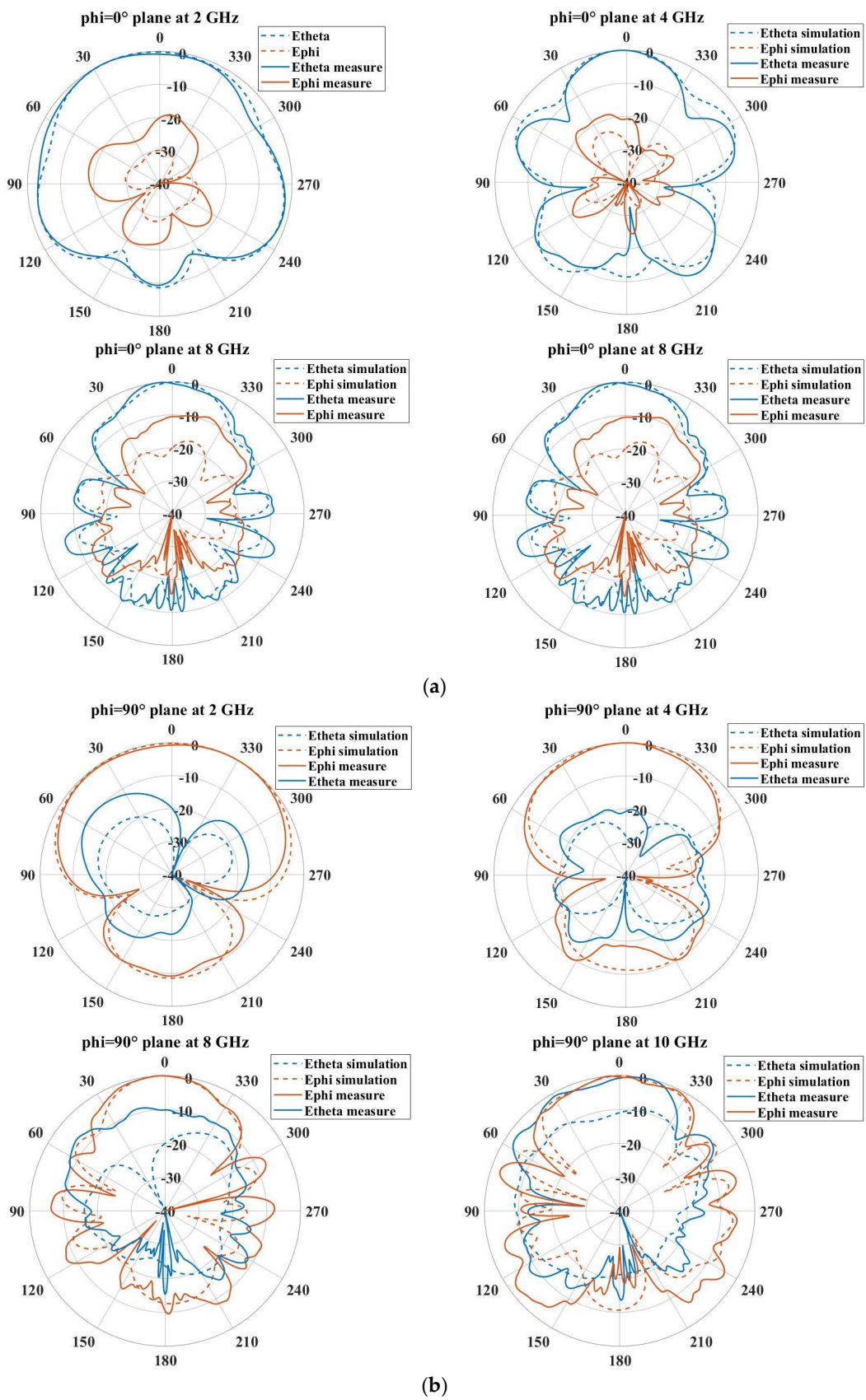


Figure 12. Simulated and measured radiation patterns in (a) $\phi = 0^\circ$ plane and (b) $\phi = 90^\circ$ plane.

The prototype of the elliptical folded dipole antenna is presented in Figure 13 and has been measured with an MVG—StarLab anechoic chamber. The simulation and measurement results show good agreement. The measured and simulated reflection coefficients are compared in Figure 11a. The measured impedance bandwidth is observed to be 2.3–26 GHz with a condition of $S_{11} < -6$ dB. The antenna satisfies the $S_{11} < -10$ dB requirement over several bands, including 3.3–8 GHz, 9.8–12.6 GHz and 13.2–26 GHz, similar to the simulation results. The measurement environment (connector, mechanical support, substrate . . .) used during measurements can explain the differences with simulation results at higher frequencies. Perhaps a connector model could also be considered during the simulation process to improve the reliability of results.

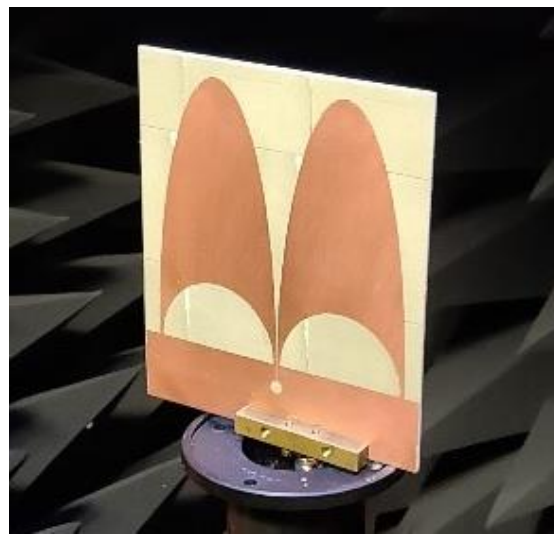


Figure 13. Photograph of the measured dipole antenna inside StarLab (MVG) anechoic chamber.

Due to the limitations of the anechoic chamber and software treatments, the efficiency is not as precise as the simulation and has consequences on the measured gain. The peak values vary from 2.9 to 8.2 dBi in the 2.3–12 GHz band. Above 12 GHz, the main beam is no longer in the broadside (z-axis) and causes a diminution of the gain in this direction such as in simulation. The measured radiation patterns show a close resemblance to the simulated ones, with the exception of higher cross-polarization values.

The radiation patterns demonstrate a directive behavior along the dipole axis (at $\theta = 0^\circ$) up to a certain frequency, as observed in the curves. However, above 12 GHz, this radiation becomes more unstable and challenging to characterize. Maybe using an even better connector could solve a part of the difference between simulations and measure above 12 GHz.

Table 2 shows that the proposed antenna provides good impedance bandwidth improvement over other folded dipole antennas [16,17,21]. Compared to other directive solutions such as tapered slots or Vivaldi antennas, the proposed design has the advantage of being reconfigurable thanks to a proper phase-shifting feeding circuit (coupling circuits, diode, switch . . .).

Table 2. Performances of the mentioned antennas and the semi-elliptical folded dipole antenna.

Reference	Type	Bandwidth (GHz)	Gain (dBi)	Reconfigurability
[9]	Square monopole	2.38–5.2	1.5–4.5	No
[16]	Folded dipole	30.3–53.7	4.6–6.7	No
[17]	Modified folded dipole	26.3–29.75	5.51	No

Table 2. Cont.

Reference	Type	Bandwidth (GHz)	Gain (dBi)	Reconfigurability
[21]	Thick Folded dipole	1.2–4.07	8.2–11.5	No
[22]	Dipole	26.5–38.2	4.5–5.8	No
[23]	Tapered slot antenna	6.2–12.3	3–6	No
[24]	Vivaldi antenna	2.9–14.2	5.5–9	No
This work	$S_{11} < -6$ dB	2.3–26	2.9–8.2	Yes
	$S_{11} < -10$ dB	3.3–8, 9.8–12.6 and 13.2–26		

5. Discussion and Conclusions

In this study, a semi-elliptical folded dipole antenna with ultra-wideband (UWB) characteristics was investigated. Thanks to an optimized dipole shape and a transition between the microstrip line and slot line, we obtain an impedance bandwidth over 167% (2.3–26 GHz) under the condition of $S_{11} < -6$ dB. This bandwidth is really wide compared to recent folded dipoles mentioned in this work. The proposed structure offers possibilities of reconfigurability through different feeding phase configurations. The study focused on the circuits that can allow such feeding, so some have not been discussed in this paper. Only the microstrip line to slot line transition, which produces a 180° phase shift feeding, has been studied here. A publication concerning only the reconfigurable aspect of the structure is envisaged. The dipole structure with a symmetrical feeding creates a directive radiation pattern. Both simulation and measurement results indicated that feeding the antenna symmetrically led to maximum gain in the broadside direction. However, cross-polarization increased at higher frequencies. The planar technology used with a common substrate makes this design a really compact and easy to integrate antenna for UWB solutions.

Author Contributions: Conceptualization, R.G. and M.H.; methodology, R.G. and M.H.; software, R.G.; validation, R.G. and M.H.; investigation, R.G. and M.H.; data curation, R.G.; writing—original draft preparation, R.G.; writing—review and editing, R.G., M.H., D.L., G.L.D., P.T. and C.L.M.; supervision, M.H., D.L., G.L.D., P.T. and C.L.M.; project administration, M.H. and G.L.D. All authors have read and agreed to the published version of the manuscript.

Funding: This research received no external funding.

Data Availability Statement: Not applicable.

Acknowledgments: This work is supported by the European Union through the European Regional Development Fund (ERDF), the Ministry of Higher Education and Research, the Région Bretagne, and through the CPER Projects 2015–2020 STIC & Ondes.

Conflicts of Interest: The authors declare no conflict of interest.

References

1. Federal Communications Commission. *First Report and Order, Revision of Part 15 of the Commission's Rules Regarding Ultra Wide Band Transmission Systems*; Federal Communications Commission: Washington, DC, USA, 2002.
2. Lorho, N.; Hubert, W.; Lestieux, S.; Chousseaud, A.; Razban, T. Bandwidth enhancement of UWB dual-polarized antennas. *Prog. Electromagn. Res. C* **2016**, *68*, 57–73. [[CrossRef](#)]
3. Mahmood, S.N.; Ishak, A.J.; Saeidi, T.; Soh, A.C.; Jalal, A.; Imran, M.A.; Abbasi, Q.H. Full Ground Ultra-Wideband Wearable Textile Antenna for Breast Cancer and Wireless Body Area Network Applications. *Micromachines* **2021**, *12*, 322. [[CrossRef](#)] [[PubMed](#)]
4. Adamiuk, G.; Zwick, T.; Wiesbeck, W. UWB Antennas for Communication Systems. *Proc. IEEE* **2012**, *100*, 2308–2321. [[CrossRef](#)]
5. Wiesbeck, W.; Adamiuk, G.; Sturm, C. Basic Properties and Design Principles of UWB Antennas. *Proc. IEEE* **2009**, *97*, 372–385. [[CrossRef](#)]
6. Ghosh, D.; De, A.; Taylor, M.; Sarkar, T.; Wicks, M.; Mokole, E.L. Transmission and Reception by Ultra-Wideband (UWB) Antennas. *IEEE Antennas Propag. Mag.* **2006**, *48*, 67–99. [[CrossRef](#)]
7. Schantz, H.G. *The Art and Science of Ultra-Wideband Antennas*; Artech House: Norwood, MA, USA, 2005.

8. Schantz, H.G. A Brief History of UWB Antennas. *IEEE AE Syst. Mag.* **2004**, *19*, 22–26. [[CrossRef](#)]
9. Ammann, M.J. Square planar monopole antenna. In Proceedings of the IEE National Conference on Antennas and Propagation, York, UK, 31 March–1 April 1999.
10. Agrawall, N.P.; Kumar, G.; Ray, K.P. Wide-band planar monopole antennas. *IEEE Trans. Antennas Propag.* **1998**, *46*, 294–295. [[CrossRef](#)]
11. Schantz, H.G. Planar elliptical element ultra-wideband dipole antennas. In Proceedings of the IEEE Antennas and Propagation Society International Symposium (IEEE Cat. No. 02CH37313), San Antonio, TX, USA, 16–21 June 2002; pp. 44–47. [[CrossRef](#)]
12. Yan, X.R.; Zhong, S.S.; Tang, X.R. Compact printed monopole antenna with extremely wide bandwidth. In Proceedings of the IET Conference on Wireless, Mobile and Sensor Networks 2007 (CCWMSN07), Shanghai, China, 12–14 December 2007; pp. 337–339.
13. Romeu, J.; Soler, J. Generalized Sierpinski fractal multiband antenna. *IEEE Trans. Antennas Propag.* **2001**, *49*, 1237–1239. [[CrossRef](#)]
14. Abdallah, M.; Colombel, F.; Le Ray, G.; Himdi, M. Quasi-Unidirectional Radiation Pattern of Monopole Coupled Loop Antenna. *IEEE Antennas Wirel. Propag. Lett.* **2009**, *8*, 732–735. [[CrossRef](#)]
15. Wang, Z.; Wu, J.; Yin, Y.; Liu, X. A Broadband Dual-Element Folded Dipole Antenna With a Reflector. *IEEE Antennas Wirel. Propag. Lett.* **2014**, *13*, 750–753. [[CrossRef](#)]
16. Xue, L.; Tan, Q.; Cheng, K.; Fan, K. A Wideband Folded Dipole Antenna with an Improved Cross-Polarization Level for Millimeter-Wave Applications. *Appl. Sci.* **2022**, *12*, 11291. [[CrossRef](#)]
17. Hwang, I.-J.; Ahn, B.; Chae, S.-C.; Yu, J.-W.; Lee, W.-W. Quasi-Yagi Antenna Array With Modified Folded Dipole Driver for mmWave 5G Cellular Devices. *IEEE Antennas Wirel. Propag. Lett.* **2019**, *18*, 971–975. [[CrossRef](#)]
18. Dubost, G.; Zisler, S. *Antenne a Large Bande Theorie et Applications*; Masson: Paris, France, 1976; pp. 175–186.
19. Guillou, L.; Daniel, J.-P.; Terret, C.; Madani, A. Rayonnement d'un Doublet Replié Epais. In *Annales Des Télécommunications*; Springer: Berlin/Heidelberg, Germany, 1975.
20. Dubost, G.; Havot, H.A. Thick Folded Dipole Which Is Tuneable within a Frequency Band of Two Octaves. U.S. Patent No. 4,005,430, 12 January 1976.
21. Dubost, G. A tuneable thick folded-dipole operating in two octaves. In Proceedings of the 1975 Antennas and Propagation Society International Symposium, Urbana, IL, USA, 3–5 June 1975; pp. 248–251.
22. Ta, S.X.; Choo, H.; Park, I. Broadband Printed-Dipole Antenna and Its Arrays for 5G Applications. *IEEE Antennas Wirel. Propag. Lett.* **2017**, *16*, 2183–2186. [[CrossRef](#)]
23. Zhang, F.; Zhang, F.S.; Zhao, G.; Lin, C.; Jiao, Y.C. A Loaded Wideband Linearly Tapered Slot Antenna With Broad Beamwidth. *IEEE Antennas Wirel. Propag. Lett.* **2011**, *10*, 79–82. [[CrossRef](#)]
24. Zhu, H.; Li, X.; Yao, L.; Xiao, J. A Novel Dielectric Loaded Vivaldi Antenna with Improved Radiation Characteristics for UWB Application. *Appl. Comput. Electromagn. Soc. J. (ACES)* **2018**, *33*, 394–399.

Disclaimer/Publisher's Note: The statements, opinions and data contained in all publications are solely those of the individual author(s) and contributor(s) and not of MDPI and/or the editor(s). MDPI and/or the editor(s) disclaim responsibility for any injury to people or property resulting from any ideas, methods, instructions or products referred to in the content.